Journal of Biophysics and Structural Biology Vol. 3(3), pp. 66-71, November 2011
Available online at http://www.academicjournals.org/jbsb
ISSN-2141-2200 ©2011 Academic Journals

Full Length Research

Crystal structure of the allosteric-defective chaperonin $GroEL_{E434K}$ mutant

Aintzane Cabo-Bilbao[1], Ariel E. Mechaly[2], Jon Agirre[1], Silvia Spinelli[3], Begoña Sot[4], Arturo Muga[1] and Diego M.A. Guérin[1]*

[1]Unidad de Biofísica (UBF, CSIC-UPV/EHU) and Departamento de Bioquímica y Biología Molecular, UPV/EHU. Barrio Sarriena s/n, E-48940, Leioa, Spain.
[2]Unité de Biochimie Structurale, Institut Pasteur, 25 rue du Dr. Roux, F-75724 Paris, France.
[3]AFMB-CNRS, UMR 6098, 163, Av. de Luminy, 13288 Marseille Cedex 09, France.
[4]Centro Nacional de Biotecnología, CSIC, Campus de la Universidad Autónoma de Madrid, Darwin, 3, 28049 Madrid, Spain.

Accepted 25 August, 2011

The chaperonin GroEL adopts a double-ring structure with various modes of allosteric communication. The simultaneous positive intra-ring and negative inter-ring cooperativities allow alternating functionality of the folding cavities in both protein rings. Mutation of glutamic acid 434 (located at the ring interface), to lysine alters the negative inter-ring cooperativity. The crystal structure of the mutant chaperonin $GroEL_{E434K}$ has been determined at low-resolution (4.5 Å) and has been compared to the wild-type GroEL and the allosteric-defective $GroEL_{E461K}$ mutant structures. Despite the allosteric-defective behavior of the $GroEL_{E434K}$mutant, its structure remains strikingly similar to that of the wild-type GroEL.

Key words: Chaperonin, GroEL, cooperativity, twinning, low-resolution refinement.

INTRODUCTION

The bacterial GroEL-GroES complex assists unfolded proteins in achieving their native conformation through an ATP-dependent cyclic reaction (Houry et al., 1999). The GroEL monomer is organized into three domains (Figure 1A): an apical domain (186 residues) that interacts with substrate proteins and its co-chaperone GroES, a flexible intermediate domain (89 residues), and an equatorial domain (243 residues) that contains the ATP binding site and is responsible for the inter-ring communication. The biological GroEL molecule is made of fourteen identical 57 kDa protomers that assemble into a stacked, double-ring structure (Figures 1B and 1C), whereas GroES is a heptamer of seven identical 10 kDa subunits arranged in a lid-like single ring (Hunt et al., 1996). The GroEL-GroES interactions and stoichiometry are dependent on the presence of Mg^{2+}, KCl, and a nonhydrolyzable ATP analogue (Gorovits et al., 1997; Llorca et al., 1997). The co-chaperone GroES alternately binds to the GroEL ring that interacts with non-native protein substrates. This process leads to isolation of the substrate in a folding chamber in which it eventually refolds into its correct conformation (Shtilerman et al., 1999). GroEL function is allosterically regulated, and both positive intra-ring and negative inter-ring cooperativities have been observed (Horovitz et al., 2001). Negative inter-ring cooperativity is thought to be mediated by, among other factors, ionic interactions at the so called 'right site' (RS) and the 'left-site' (LS) of the inter-ring interface. These interactions involve residues Glu461 and Arg452 (Bartolucci et al., 2005; PDB 1XCK) at the RS and the putative salt bridge between Glu434 and Lys105 (Llorca et al., 1997; Sot et al., 2003) at the LS. Mutation of residues Glu461 and Glu434 to lysine affects the ability of GroEL to distinguish between physiological and stress temperatures (Sot et

*Corresponding author. E-mail: diego.guerin@ehu.es

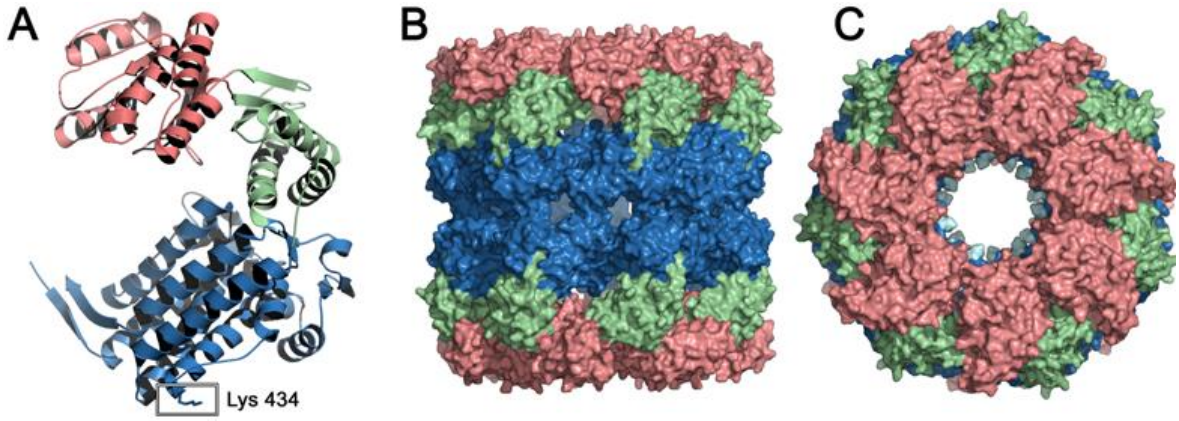

Figure 1. Overall structure. (A) Ribbon diagram of a $GroEL_{E434K}$ protomer, which consists of three functionally distinct domains: an apical domain (residues 189–377), an intermediate domain (residues 137–188 and 378–409) and an equatorial domain (residues 2-136 and 410-425). (B) Side view of the GroEL complex, consisting of two stacked homo-heptameric rings. (C) Each ring is formed by seven identical protomers. View along the 7-fold symmetry axis

al., 2002; 2003), and also decrease the chaperoning ATPase activity at 25°C (Sot et al., 2002). Up to date there is no structural information available on either of these two GroEL single mutants in complex with nucleotides. To better understand the role of the inter-ring interactions in the chaperonin inter-ring negative cooperativity, we have studied two allosteric-defective mutants, $GroEL_{E461K}$ and $GroEL_{E434K}$. We have previously determined the crystal structure of $GroEL_{E461K}$ (Cabo-Bilbao et al., 2006) (PDB 2EU1). Here we report a 4.5 Å resolution structure of $GroEL_{E434K}$ from perfect hemihedral twinned crystals.

MATERIALS AND METHODS

Protein expression and purification

Purification of $GroEL_{E434K}$ was carried out following a previously described protocol (Weissman et al., 1995). The GroEL mutant protein was produced in *E. coli* cells transformed with the plasmid pOF39, which causes overexpression of both GroEL and GroES in the bacteria (Fayet et al., 1986; 1989). Cells were grown in LB medium supplemented with chloramphenicol (25 µg/ml) at 37°C until A_{550} = 0.5. Overexpression was induced with 0.5 mg/ml arabinose for 4 h.

Cells were harvested by centrifugation and resuspended in 5 mM EDTA, 1 mM DTT, 1 mM PMSF, 50 mM Tris-HCl at pH 7.5, and 200 µg/ml lysozyme. After disrupting the cells by sonication, the lysate was centrifuged at 10,000 g for 1 h. The supernatant was precipitated with 70% (w/v) ammonium sulfate for 4 h at 4°C and centrifuged for 20 min at 15,000 g. The pellet was resuspended in 50 mM Tris-HCl at pH 7.5, 1 mM EDTA, 1 mM DTT, and 1 mM PMSF and then dialyzed against the same buffer. The sample was loaded into an ion exchange FPLC column (Q-Sepharose High Performance 26/20) previously equilibrated with 1 mM EDTA, 1 mM DTT and 50 mM Tris-HCl at pH 7.5 and then washed at a rate of 3 ml/min with two column volumes of the equilibration buffer. The protein was eluted with five column volumes using a NaCl gradient from 0 to 1 M at a flow rate of 2 ml/min. Fractions containing $GroEL_{E434K}$ were concentrated by ultrafiltration in Centricon YM-100 filters (Millipore, Bedford M.A., U.S.A) up to 50 mg/ml and washed three times with 10 mM $MgCl_2$ and 50 mM Tris-acetate at pH 8.0 to eliminate most of the lower molecular weight contaminants. Other contaminants that co-purified bound to $GroEL_{E434K}$ were eliminated in a final step. The protein (2-10 mg/ml) was injected into a Reactive Red 120-Agarose (Sigma, St. Louis, MO, U.S.A.) column equilibrated with 5 mM $MgCl_2$ and 20 mM Tris-HCl at pH 7.5 and then eluted with 15 column volumes of 1.5 M NaCl, 0.02% NaN_3, and 20 mM Tris-HCl at pH 7.5 (Clark et al., 1998).

Crystallization, X-ray data collection and processing

Screening of crystallization conditions was carried out using a Mosquito nano-drop dispensing robot (TTP Labtech, UK). Micro-crystals grew at 4°C for two days in a drop equilibrated in a 50 µL reservoir containing the following precipitant solution: 1.2 M NaH_2PO_4, 0.8 M K_2HPO_4, 200 mM $LiSO_4$, and 100 mM CAPS at pH 10.5 (Appendix).

Larger crystals were grown by the hanging-drop vapor diffusion method at 4°C in the above-mentioned conditions, and slight modifications were made to either the pH, precipitant or protein concentration for improved growth in Linbro plates (Appendix). These crystals were dehydrated by incubating the drops containing the crystals in vapor diffusion equilibrium with increasing concentrations of Li_2SO_4. Finally, 4 M NaH_2PO_4 was employed as a cryoprotectant.

Diffraction data were collected at beamline ID14-1 at the European Synchrotron Radiation Facility (ESRF), France. Data were indexed and integrated using the Mosflm program (Leslie, 1992). Scaling and merging of the data were done with SCALA from the CCP4 suite (Collaborative Computational Project, 1994).

Structure determination and refinement

The $GroEL_{E434K}$ atomic structure was determined by molecular replacement using Phaser (McCoy et al., 2007), employing one ring (one heptamer) of the wild-type apo-chaperonin (PDB code: 1XCK)

Table 1. Data collection and refinement statistics. Values between parentheses are for the highest resolution shell. [1] $R_{merge} = \sum_{hkl} \sum_i | I_i(hkl) - \langle I_i(hkl) \rangle | / \sum_{hkl} \sum_i I_i(hkl)$, being $I_i(hkl)$ the intensity of the *hkl* reflection and *i* the number of measurements of that reflection. [2] $R_{work} = \sum_{hkl} | F_{obs} - F_{calc} | / \sum_{hkl} | F_{obs} |$, being F_{obs} and F_{calc} the observed and calculated structure factors respectively. [3] R_{free} = R-value calculated for the 5% of reflections not used in the refinement process.

Data collection	
Unit-cell parameters (Å)	a=b= 172.0 c= 454.6
Space group	$P3_2$
Resolution range (Å)	20.0-4.5 (4.74-4.50)
No. of observations	252,352 (37,848)
No. of number unique observations	87,597 (13,001)
Mean I/σ(I)	6.0 (2.3)
Completeness	98.2 (99.7)
Multiplicity	2.9 (2.9)
R_{merge} [1]	0.150 (0.472)
Refinement	
R_{work} [2]/R_{free} [3]	0.17/0.24
No. of protein atoms	53,984
Average B factor	174.112
R.m.s.d. for bond lengths (Å)	0.03
R.m.s.d. for bond angles (°)	2.3
Ramachandran favored, residues in (%)	95.9
Ramachandran outliers, residues in (%)	1.2
Rotamers outliers, residues in (%)	1.9

as a search model. A clear solution containing two heptameric rings per asymmetric unit (log-likelihood gain = 7923.440) was found in space group $P3_2$. However, initial refinement attempts with the program phenix. refine (Afonine et al., 2005) failed, suggesting the presence of twinned data. Twinning was confirmed by analyzing the diffraction data with phenix. xtriage (Adams et al., 2010), as L and N(z) tests showed that the intensities from our dataset clearly deviated from the expected values for untwinned data. Application of the twinning law "h,-h-k,-l" allowed the refinement to proceed to completion. Refinement included TLS groups and restraints for NCS (14-fold) secondary structure, Ramachandran angles and the reference model (PDB code: 1XCK). Minor manual modifications to the model between refinement rounds were done using the program COOT (Emsley and Cowtan, 2004; Emsley et al., 2010). The final model of the $GroEL_{E434K}$ mutant was refined until a crystallographic R_{work} and R_{free} of 0.17 and 0.24 were reached, respectively (Table 1). Figures were prepared using the program PyMOL (DeLano, 2002). Atomic coordinates and structure factors of $GroEL_{E434K}$ have been deposited in the RCSB Protein Data Bank with the accession code 2YEY.

RESULTS AND DISCUSSION

Overall structure

Here we report the X-ray structure of the $GroEL_{E434K}$ allosteric-defective mutant (Sot et al., 2003) determined at 4.5 Å resolution from hemihedral twinned crystals. Despite the limited resolution of the data, modern refinement software (Brunger et al., 2009; Schroder et al., 2010; Read, 2010) allows to determine the atomic structure accurately. In order to obtain a reliable model in terms of both secondary structure and crystallographic R factors, we used several restraints in the phenix. refine program. These restraints were as follows:

(i) 14-fold NCS,
(ii) The wild-type GroEL structure (PDB code 1XCK) as a reference model,
(iii) Ramachandran restraints.

The $GroEL_{E434K}$ crystal structure does not show any major structural differences when compared to the wild-type apo structure (Bartolucci et al., 2005) (PDB code 1XCK). When these structures are superimposed by their Cα, backbones, the r.m.s.d is approximately 0.5 Å. It is noteworthy that the $GroEL_{E434K}$ structure was determined in an unrelated crystalline environment as compared with the wild-type structure. Consequently, we conclude that crystal packing does not force the wild-type-like relative orientation of the rings.

Inter-ring interface

In our previously reported crystal structure of the allosteric-defective variant $GroEL_{E461K}$ (PDB code 2EU1), we observed a rotation of 22° between rings relative to

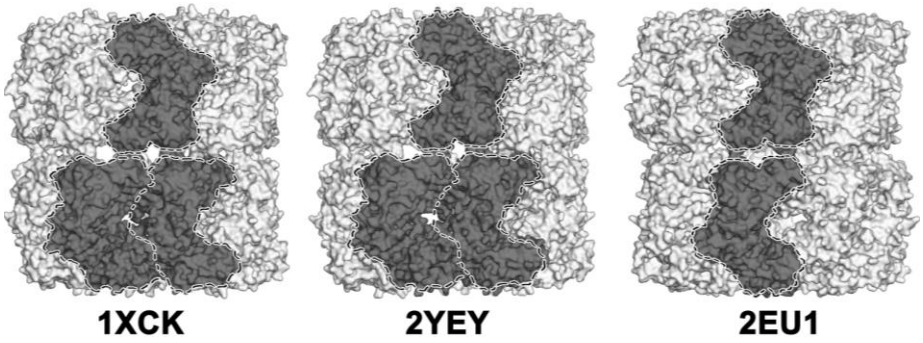

Figure 2. Comparison between wild-type GroEL, $GroEL_{E434K}$ and $GroEL_{E461K}$ mutants. In both wild-type GroEL (PDB 1XCK) and $GroEL_{E434K}$ (PDB 2YEY), each protomer contacts two protomers at the opposing ring (1:2 contact). In contrast, in the $GroEL_{E461K}$ mutant (PDB 2EU1), the upper ring is rotated 22° about the 7-fold axis, and consequently each protomer contacts only one protomer at the opposite ring (1:1 contact).

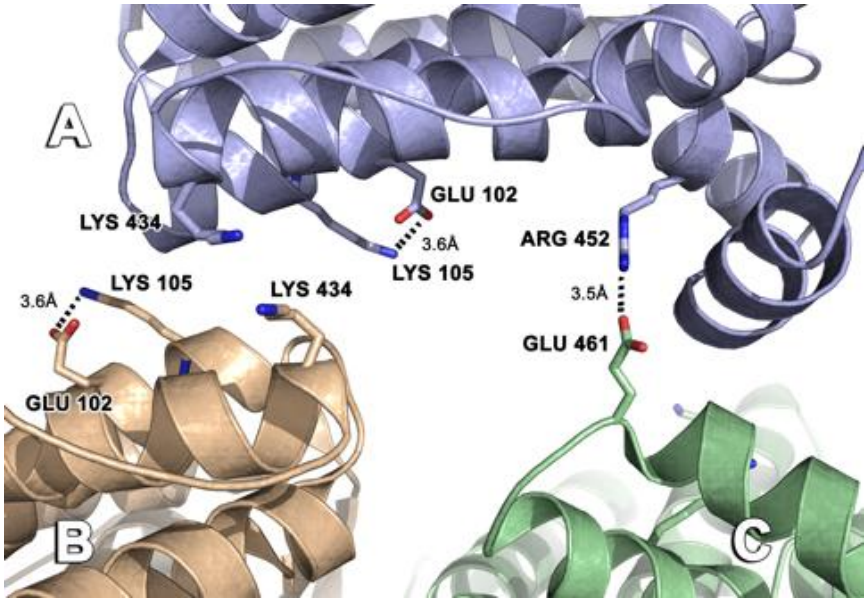

Figure 3. Ring interface of the $GroEL_{E434K}$ mutant. The top monomer is labeled 'A', while left and right contact sites are labeled 'B' and 'C,' respectively. There is a salt bridge between arginine 452 of the top monomer (A) and glutamic acid 461 of the right bottom monomer (C).

the wild-type GroEL structure (Bartolucci et al., 2005). In the structure of that mutant, we observed that the interface was not stabilized by any inter-ring salt bridges and that the inter-ring distance was slightly larger than that of the wild-type GroEL (Cabo-Bilbao et al., 2006). Despite also having its inter-ring communication altered, the $GroEL_{E434K}$ mutant maintains the same interface (1:2 contact) observed in the wild-type chaperonin (Figure 2), in contrast to the $GroEL_{E461K}$ mutant.

The replacement of glutamic acid 434 with lysine modifies the surface charge distribution of the inter-ring interface. A strong bend of lysines from both the top and bottom monomers is observed (Figure 3), which most likely occurs as a consequence of electrostatic repulsions between the positively charged side-chains on residues 434 on each monomer. Nevertheless, this repulsive effect is not strong enough to disrupt the salt bridge formed between Arg452 and Glu461 at the RS (Figure 3), which is the major inter-ring interaction in the wild-type GroEL structure (Bartolucci et al., 2005). Consequently, this salt bridge might be essential for the conservation of the 1:2 contact between opposing rings in the $GroEL_{E434K}$ variant.

Our results are consistent with the previously determined structure of the double mutant $GroEL_{D398A-E434A}$ (Wang and Boisvert, 2003) (PDB codes 1KP8 and 1J4Z), in which no major changes in the inter-ring interface were observed. It is interesting to note that while the functional effects of the E461K and E434K mutations are similar, i.e., they switch from a foldase to a holdase activity at 32 and 29°C, respectively (Sot et al., 2003), their respective inter-ring interfaces differ significantly. Thus, different molecular mechanisms might disrupt inter-ring allosteric signaling in these GroEL variants to render them inactive as foldases at physiological temperatures.

Conclusion

Although the low resolution of the data prevents a deeper structural analysis, we can conclude that, in agreement with previously determined GroEL structures containing mutations in residue E434, the E434K mutation does not seem to cause any obvious structural change with respect to the wild-type GroEL structure. From this study, we can conclude that in contrast to what we observed from the E461K mutant (Cabo-Bilbao et al., 2006), the communication pathway through the LS can be interrupted without inducing major changes at the inter-ring interface. Consequently, these results suggest that the communication pathway through this contact site most likely occurs by small structural modifications rather than large conformational changes.

ACKNOWLEDGMENTS

We acknowledge the European Synchrotron Radiation Facility (ESRF) for providing access to X-ray sources and the ID14-1 staff for support and assistance in data collection. A.C-B. and J.A. received fellowships from the Basque Government, and A.E.M. received a fellowship from the MEyC, Spain. D.M.A.G. is researcher from the Fundación Biofísica Bizkaia who received partial support from Bizkaia::Xede, Bizkaia, Basque Country, Spain. Part of this project was funded by ETORTEK, FEDER, MEC (BFU2010-15443), and the Basque Government (IT-358-07).

REFERENCES

Adams PD, Afonine PV, Bunkoczi G, Chen VB, Davis IW, Echols N, Headd JJ, Hung LW, Kapral GJ, Grosse-Kunstleve RW, McCoy AJ, Moriarty NW, Oeffner R, Read RJ, Richardson DC, Richardson JS, Terwilliger TC, Zwart PH (2010). PHENIX: a comprehensive Python-based system for macromolecular structure solution. Acta Crystallogr. D. Biol. Crystallogr., 66:213-221

Afonine PV, Grosse-Kunstleve RW, Adams PD (2005). A robust bulk-solvent correction and anisotropic scaling procedure. Acta.Crystallogr. D. Biol. Crystallogr., 61:850-855

Bartolucci C, Lamba D, Grazulis S, Manakova E, Heumann H (2005). Crystal structure of wild-type chaperonin GroEL. J. Mol. Biol., 354:940-951

Brunger AT, DeLaBarre B, Davies JM, Weis WI (2009). X-ray structure determination at low resolution. Acta. Crystallogr. D. Biol. Crystallogr., 65:128-133

Cabo-Bilbao A, Spinelli S, Sot B, Agirre J, Mechaly AE, Muga A, Guerin DM (2006). Crystal structure of the temperature-sensitive and allosteric-defective chaperonin GroELE461K. J. Struct. Biol., 155:482-492

Clark AC, Ramanathan R, Frieden C (1998). Purification of GroEL with low fluorescence background. Methods Enzymol., 290:100-118

Collaborative Computational Project N (1994). The CCP4 suite: programs for protein crystallography. Acta. Crystallogr. D. Biol. Crystallogr., 50:760-763

DeLano WL (2002). The PYMOL Molecular Graphics System.

Emsley P, Cowtan K (2004). Coot: model-building tools for molecular graphics. Acta. Crystallogr. D. Biol. Crystallogr., 60:2126-2132

Emsley P, Lohkamp B, Scott WG, Cowtan K (2010). Features and development of Coot. Acta. Crystallogr. D.Biol. Crystallogr., 66:486-501

Fayet O, Louarn JM, Georgopoulos C (1986). Suppression of the *Escherichia coli* dnaA46 mutation by amplification of the groES and groEL genes. Mol. Gen. Genet., 202:435-445

Fayet O, Ziegelhoffer T, Georgopoulos C (1989). The groES and groEL heat shock gene products of Escherichia coli are essential for bacterial growth at all temperatures. J. Bacteriol., 171:1379-1385

Gorovits BM, Ybarra J, Seale JW, Horowitz PM (1997). Conditions for nucleotide-dependent GroES-GroEL interactions. GroEL14(groES7)2 is favored by an asymmetric distribution of nucleotides. J. Biol. Chem., 272:26999-27004

Horovitz A, Fridmann Y, Kafri G, Yifrach O (2001). Review: allostery in chaperonins. J. Struct. Biol., 135:104-114

Houry WA, Frishman D, Eckerskorn C, Lottspeich F, Hartl FU (1999). Identification of in vivo substrates of the chaperonin GroEL. Nature 402:147-154

Hunt JF, Weaver AJ, Landry SJ, Gierasch L, Deisenhofer J (1996). The crystal structure of the GroES co-chaperonin at 2.8 A resolution. Nature, 379:37-45

Leslie AGW (1992). Recent changes to the MOSFLM package for processing film and image plate data. Joint CCP4 + ESF-EAMCB Newsletter on Protein Crystallography, 26:7

Llorca O, Perez-Perez J, Carrascosa JL, Galan A, Muga A, Valpuesta JM (1997). Effects of the inter-ring communication in GroEL structural and functional asymmetry. J. Biol. Chem., 272:32925-32932

McCoy AJ, Grosse-Kunstleve RW, Adams PD, Winn MD, Storoni LC, Read RJ (2007). Phaser crystallographic software. J. Appl. Crystallogr., 40:658-674

Read RJ (2010). From poor resolution to rich insight. Structure, 18:664-665

Schroder GF, Levitt M, Brunger AT (2010). Super-resolution biomolecular crystallography with low-resolution data. Nature, 464:1218-1222

Shtilerman M, Lorimer GH, Englander SW (1999). Chaperonin function: folding by forced unfolding. Science, 284:822-825

Sot B, Galan A, Valpuesta JM, Bertrand S, Muga A (2002). Salt bridges at the inter-ring interface regulate the thermostat of GroEL. J. Biol. Chem., 277:34024-34029

Sot B, Banuelos S, Valpuesta JM, Muga A (2003). GroEL stability and function. Contribution of the ionic interactions at the inter-ring contact sites. J. Biol. Chem., 278:32083-32090

Wang J, Boisvert DC (2003). Structural basis for GroEL-assisted protein folding from the crystal structure of (GroEL-KMgATP)14 at 2.0A resolution. J. Mol. Biol., 327:843-855

Weissman JS, Hohl CM, Kovalenko O, Kashi Y, Chen S, Braig K, Saibil HR, Fenton WA, Horwich AL (1995). Mechanism of GroEL action: productive release of polypeptide from a sequestered position under GroES. Cell, 83:577-587.

Appendix

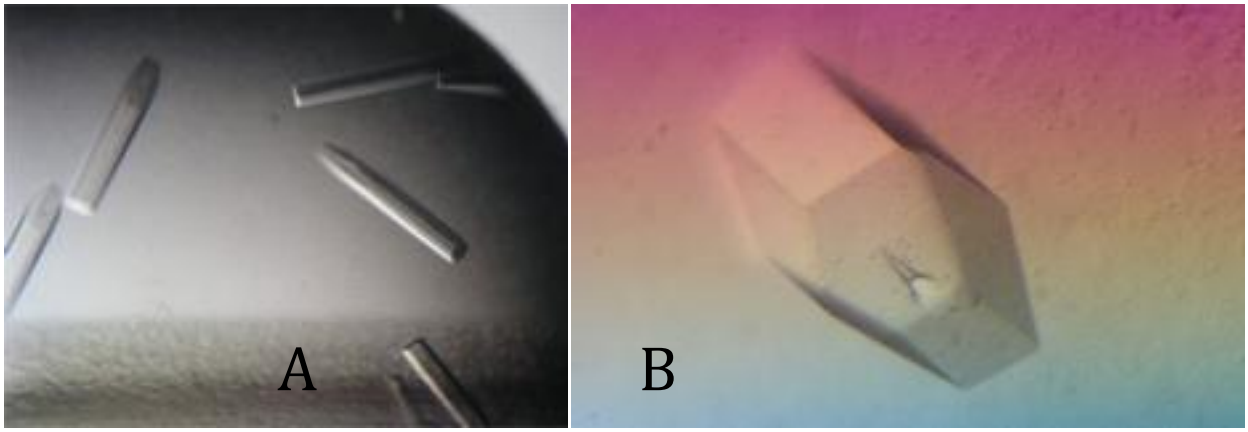

(A) Photograph of initial $GroEL_{E434K}$ crystals. Crystals were grown in a half height Greiner Crystal Ledge Plate. The longest crystal size was approximately 0.01 mm. (B) Photograph of an improved **$GroEL_{E434K}$ crystal.** Crystals were grown in a Linbro plate employing the hanging drop vapor diffusion method. Crystal size is 0.05 mm.